Kelleher, D. J., Dudycz, L. W., Wright, G. E., & Johnson, G. L. (1986) *Mol. Pharmacol. 30*, 603–608.
Kuhn, H. (1981) *Curr. Top. Membr. Transp. 15*, 171–201.
Lochrie, M. A., Hurley, J. B., & Simon, M. I. (1985) *Science (Washington, D.C.) 228*, 96–99.
Manning, D. R., & Gilman, A. G. (1983) *J. Biol. Chem. 258*, 7059–7063.
Medynski, D. C., Sullivan, K., Smith, D., Van Dop, C., Chang, F.-H., Fung, B. K.-K., Seeburg, P. H., & Bourne, H. R. (1985) *Proc. Natl. Acad. Sci. U.S.A. 82*, 4311–4315.
Neer, E. J., Lok, J. M., & Wolf, L. G. (1984) *J. Biol. Chem. 259*, 14222–14229.
Northup, J. K., Smigel, M. D., & Gilman, A. G. (1982) *J. Biol. Chem. 257*, 11416–11423.
Northup, J. K., Smigel, M. D., Sternweis, P. C., & Gilman, A. G. (1983) *J. Biol. Chem. 258*, 11369–11376.
Nukada, T., Tanabe, T., Takahashi, H., Noda, M., Hirose, T., Inayama, S., & Numa, S. (1986) *FEBS Lett. 195*, 220–224.
Robishaw, J. D., Russell, D. W., Harris, B. A., Smigel, M. D., & Gilman, A. G. (1986) *Proc. Natl. Acad. Sci. U.S.A. 83*, 1251–1255.
Roof, D. J., Applebury, M. L., & Sternweis, P. C. (1985) *J. Biol. Chem. 260*, 16242–16249.
Shinozawa, T., Uchida, S., Martin, E., Cafiso, D., Hubbell, W., & Bitensky, M. (1980) *Proc. Natl. Acad. Sci. U.S.A. 77*, 1408–1411.
Sternweis, P. C., & Robishaw, J. D. (1984) *J. Biol. Chem. 259*, 13806–13813.
Sternweis, P. C., Northup, J. K., Smigel, M. D., & Gilman, A. G. (1981) *J. Biol. Chem. 256*, 11517–11526.
Stryer, L., Hurley, J. B., & Fung, B. K.-K. (1981) *Curr. Top. Membr. Transp. 15*, 93–108.
Sugimoto, K., Nukada, T., Tanabe, T., Takahashi, H., Noda, M., Minamino, N., Kangawa, K., Matsuo, H., Hirose, T., Inayama, S., & Numa, S. (1985) *FEBS Lett. 191*, 235–240.
Sunyer, T., Codina, J., & Birnbaumer, L. (1984) *J. Biol. Chem. 259*, 15447–15451.
Tanabe, T., Nukada, T., Nishikawa, Y., Sugimoto, K., Suzuki, H., Takahashi, H., Noda, M., Haga, T., Ichiyama, A., Kangawa, K., Minamino, N., Matsuo, H., & Numa, S. (1985) *Nature (London) 315*, 242–245.
Watkins, P. A., Burns, D. L., Kanaho, Y., Liu, T.-Y., Hewlett, E. L., & Moss, J. (1985) *J. Biol. Chem. 260*, 13478–13482.
Weiss, E. R., Hadcock, J. R., Johnson, G. L., & Malbon, C. C. (1987) *J. Biol. Chem. 262*, 4319–4323.
Wessling-Resnick, M., & Johnson, G. L. (1987) *J. Biol. Chem. 262*, 3697–3705.
Yamanaka, G., Eckstein, F., & Stryer, L. (1985) *Biochemistry 24*, 8094–8101.
Yamanaka, G., Eckstein, F., & Stryer, L. (1986) *Biochemistry 25*, 6149–6153.
Yamazaki, A., Stein, P. J., Chernoff, N., & Bitensky, M. W. (1983) *J. Biol. Chem. 258*, 8188–8194.
Yatsunami, K., & Khorana, H. G. (1985) *Proc. Natl. Acad. Sci. U.S.A. 82*, 4316–4320.
Yatsunami, K., Pandya, B. V., Oprian, D. D., & Khorana, H. G. (1985) *Proc. Natl. Acad. Sci. U.S.A. 82*, 1936–1940.

Denaturation and Renaturation Studies of Benzo[*a*]pyrene Metabolite Modified DNAs†

Fu-Ming Chen
Department of Chemistry, Tennessee State University, Nashville, Tennessee 37203
Received December 11, 1986; Revised Manuscript Received March 11, 1987

ABSTRACT: Evidence from absorbance, fluorescence, and circular dichroism (CD) measurements strongly suggests that adduct conformations at the binding sites are grossly different before and after thermal denaturation of (+)-*trans*-7,8-dihydroxy-*anti*-9,10-epoxy-7,8,9,10-tetrahydrobenzo[*a*]pyrene [(+)-*anti*-BPDE] modified DNAs. This conclusion is reached through the following observations: (1) upon melting and cooling, the (+)-*anti*-BPDE-modified DNA exhibits pronounced hypochromic effects with concomitant spectral red shifts for the pyrenyl absorbance; (2) the pyrenyl CD spectrum reverses sign upon thermal denaturation–renaturation; (3) the fluorescence emission spectra resulting from excitations at 353 nm (10 nm to the red of hydrolyzed and unbound *anti*-BPDE) exhibit enhanced intensities and spectral red shifts for the thermally denatured and cooled adducts; and (4) in contrast to the absence of a shoulder prior to melting, the postmelt adducts exhibit a prominent 355-nm maximum (evidence of stacking interactions) in the excitation spectrum when 384–387-nm emission is monitored. Studies with synthetic polynucleotides further reveal that (+)-*anti*-BPDE-modified poly(dG)·poly(dC) exhibits the greatest nonreversible renaturation at the binding sites, possibly as a consequence of pyrenyl self-stacking. This, coupled with the previous findings that this polymer suffers the most extensive (+)-*anti*-BPDE modification, appears to suggest that $(dG)_n$·$(dC)_n$ regions may be responsible for such observed effects in native DNA.

Covalent modification of DNA by reactive metabolites is generally believed to be the initial critical event in the carcinogenesis of some polycyclic aromatic hydrocarbons (PAHs) (Harvey, 1981). There is strong evidence to suggest that the ultimate carcinogenic metabolite of benzo[*a*]pyrene (BP), the most widely studied PAH, is (+)-*trans*-7,8-dihydroxy-*anti*-9,10-epoxy-7,8,9,10-tetrahydrobenzo[*a*]pyrene [(+)-*anti*-BPDE] (Brookes & Osborne, 1983; Conney, 1982; Newbold et al., 1979). This metabolite is strongly guanine specific as

† Research supported by USPHS Grant CA-42682 and by a subproject of MBRS Grant S06RR0892.

0006-2960/87/0426-4323$01.50/0

well as stereospecific (Meehan & Straub, 1979), with the dominant covalent adduct resulting from trans addition of the exocyclic amino group of guanine to the C10 position of *anti*-BPDE (Weinstein et al., 1976; Jeffrey et al., 1977; Moore et al., 1977). Spectroscopic studies reveal that the DNA covalent adducts of (+)-*anti*-BPDE are, to a large extent, not intercalative in nature (Geacintov et al., 1976, 1978, 1980; Lefkowitz & Brenner, 1982). The externally situated pyrenyl moiety does not exhibit strong stacking interactions with the DNA bases, as judged from a mere 2–3-nm spectral red shift. The predominant external nature of the (+)-*anti*-BPDE covalent adducts is distinct from the significant intercalative contributions (and lower level of covalent modification) found in adducts of (−)-*anti*-BPDE (Geacintov et al., 1984) and *syn*-BPDE (Undeman et al., 1983). This has led to the suggestion that the carcinogenic potency of the (+) enantiomer may result from its higher reactivity toward DNA as well as its ability to form predominantly external covalent adducts (Geacintov et al., 1984).

Since it is reasonable to assume that physical binding preceeds covalent lesion, the formation of predominant external DNA covalent adducts by (+)-*anti*-BPDE is puzzling in view of the fact that its physical binding to DNA is predominantly intercalative in nature (Geacintov et al., 1981; Meehan et al., 1982). Such discrepancies between the physical and chemical binding modes have led to the proposal that covalent lesion occurs initially at the intercalative site and then is subsequently reoriented to an external environment (Geacintov, 1985). If such a reorientation does occur, it most likely involves local denaturation (and possibly renaturation) (Miller et al., 1985) at the binding sites. Thus, a corollary to the reorientation model appears to be that the conformation with the pyrenyl moiety at the external site is the energetically favorable conformation after denaturation and renaturation processes. If this is indeed the case, then one would expect that the thermal denaturation and renaturation of the *anti*-BPDE-modified DNA would return the modified DNA to the original premelt conformation at the binding site (i.e., external moiety with little stacking interactions). The study presented here investigates this conformational model by denaturation experiments, utilizing a variety of spectroscopic techniques including absorption, fluorescence, and circular dichroism (CD). Polynucleotides of defined sequences are also employed to delineate the possible sequence dependence of such effects.

Materials and Methods

Salmon testes DNA (ST-DNA) was purchased from Sigma, and an extinction coefficient of 6550 M^{-1} cm^{-1} at 260 nm has been used for its concentrations (per nucleotide) determination. A 0.1 mM solution of this DNA in 10 mM tris(hydroxymethyl)aminomethane hydrochloride (Tris-HCl) buffer of pH 8 containing 0.01 M NaCl exhibits a 37% thermal hyperchromicity. Sources and values of extinction coefficients for the other polynucleotides have been described earlier (Chen, 1983, 1986). Enantiomers of *anti*-BPDE were purchased from NCI Chemical Carcinogen References Standard Repository, a function of the Division of Cancer Cause and Prevention, NCI, NIH, Bethesda, MD. Stock solutions of (+)-*anti*-BPDE (4.56 mM) and (−)-*anti*-BPDE (4.06 mM) were prepared in tetrahydrofuran containing about 2% (v/v) triethylamine, and the *anti*-BPDE concentrations were determined by using an extinction coefficient (in 95% ethanol) of 48 600 M^{-1} cm^{-1} at 344 nm.

Covalently modified DNA solutions were prepared by adding aliquots of *anti*-BPDE stock solution to amber vials containing 2.3 mL of 0.1 mM DNA solutions to result in final *anti*-BPDE concentrations of 25 μM. The mixtures were then incubated overnight at 25 °C to ensure complete reaction. The reacted mixture was then applied to a 9 × 300 mm column containing Sephadex G-150 medium that had been preequilibrated with the elution buffer (10 mM Tris-HCl with 10 mM NaCl, same as in the DNA solution preparation), and fractions were collected. Base line separation is achieved with DNA fractions peaked around an elution volume of 6 mL in contrast to about 30 mL for the BP-tetraols, with a flow rate of around 3 mL/h. The DNA concentrations were determined after appropriate corrections were made for the absorbance contribution from the covalently bound *anti*-BPDE, taking into account the spectral shifts [see Chen (1986) for details]. The concentration of the covalently bound *anti*-BPDE was determined by the absorbance intensity in the 342–346-nm region by utilizing an extinction coefficient of 29 000 M^{-1} cm^{-1} (Weinstein et al., 1976). Pyrenyl absorbance intensities at temperatures above melting were used for the bound *anti*-BPDE concentration determination to minimize possible errors introduced by a hypochromic effect due to stacking interactions with the bases, except for the few cases where thermal melting results in a hypochromic effect.

Absorption spectra were measured with a Cary 210 spectrophotometric system with cuvettes of 1-cm path length. CD spectra were obtained with a Jasco J-500A recording spectropolarimeter at appropriate temperatures. Fluorescence spectra were measured at room temperature with a Jasco PF-550 fluorometer using a semimicro cell. All fluorescence measurements were made with excitation and emission slit widths of 3 and 5 nm, respectively, and spectra are not corrected. To minimize the sample exposure to light, scan rates of 50 nm/min were used in all fluorescence measurements. Absorption and CD spectra presented have been normalized to 0.1 mM DNA concentration. Melting experiments were performed in stoppered quartz cuvettes by using the "chart" utility of the temperature readout accessory of the Cary 210 with a 0.5 °C/min heating rate maintained by a Neslab RTE-8 refrigerated circulating bath and an EPT-4RC temperature programmer. The melted solutions were then returned to room temperature with approximately 1 °C/min cooling rates.

Results

Anti-BPDE-Modified Natural DNA

Absorption Spectral Evidence Indicates Denaturation Enhances Pyrenyl Stacking Interactions. It has been reasonably well established through various techniques that the appearance of a 353-nm maximum (10 nm red shifted from the 343-nm maximum of BP-tetraols) is associated with the intercalative binding of a planar pyrenyl moiety to DNA (Meehan et al., 1982; Geacintov et al., 1981; MacLeod & Selkirk, 1982). The pyrenyl absorption spectra for the (+)-*anti*-BPDE-modified DNA during a thermal denaturation cycle are shown in Figure 1A. Prior to melting, the pyrenyl absorbance maxima for the adducts are seen at 345 and 328 nm. Thermal denaturation, however, results in pyrenyl absorbance reductions with concomitant spectral broadening and red shifts. Instead of a return to the original spectrum, further red shifts (350- and 333-nm maxima) and absorbance reductions are observed upon cooling back to room temperature. These observations are consistent with earlier racemic *anti*-BPDE results showing a 351-nm absorption maximum in the postdenaturation spectrum which has been classified as type III complex (Undeman et al., 1983).

The premelt absorption spectrum of the (−)-*anti*-BPDE-modified DNA also exhibits a 345-nm maximum but with

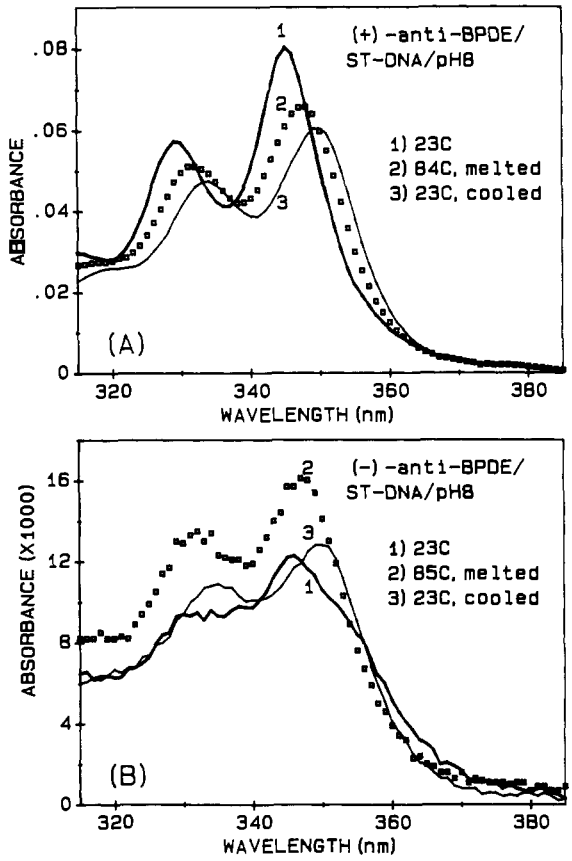

FIGURE 1: Pyrenyl absorption spectra of *anti*-BPDE-modified ST-DNA during a thermal denaturation cycle. Tris-HCl buffer (10 mM) of pH 8 containing 10 mM NaCl and 1 mM EDTA is used throughout. All absorption and CD spectra have been measured with 1-cm path length cells and normalized to 0.1 mM DNA concentation. (A) 2.6% (+)-*anti*-BPDE modified (26 DNA bases out of 1000 are attached to BPDE); (B) 0.6% (−)-*anti*-BPDE modified.

much reduced intensity (Figure 1B), a consequence of the lower level of covalent modification. Spectral broadening around 355 nm, however, is quite apparent. This suggests increased relative importance of the intercalative mode of binding, possible as a consequence of reduced external binding contribution. In contrast to the hypochromic effect of the (+) enantiomer, the (−)-*anti*-BPDE adducts exhibit absorbance enhancement upon melting. The pyrenyl hyperchromic effect upon denaturation is consistent with the significant intercalative covalent binding of the (−) enantiomer to the duplex DNA as shown by linear dichroism (Geacintov et al., 1984). Upon cooling to room temperature, however, the absorbance maximum is red-shifted, without returning to the original 345-nm maximum. The pre- and postmelt spectral differences of the (−) adducts, however, are not as dramatic as those of the (+) enantiomer, possibly as a consequence of significant intercalative contributions of the (−)-*anti*-BPDE adducts which return to the same intercalative conformation upon renaturation.

The hypochromic effects observed in the absorption spectra along with accompanying red shifts are characteristic of strong stacking interactions. These observations are consistent with the enhanced stacking interactions of the pyrenyl moiety with the bases upon denaturation and cooling. The pyrenyl spectral irreversibility indicates that upon denaturation significant portions of adducts fail to return to the original conformations at the binding sites.

Gross Adduct Conformational Differences As Revealed by CD. The pre- and postmelt CD spectra for the (+)-*anti*-BPDE-modified DNA at ambient temperature are shown in

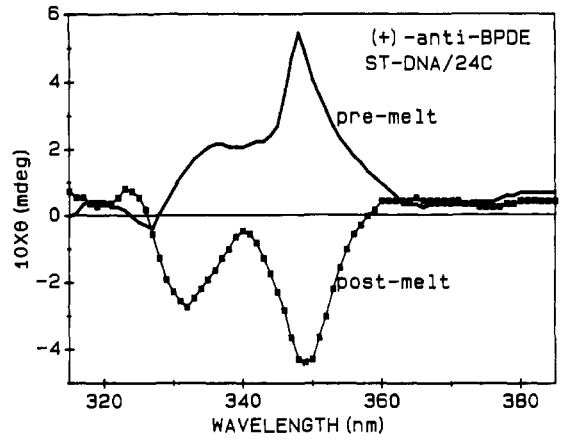

FIGURE 2: Comparison of pre- and postmelt CD spectra at room temperature of 2.6% (+)-*anti*-BPDE-modified ST-DNA.

Figure 2. Prior to melting, the adducts exhibit a positive pyrenyl CD maximum at 348 nm. A dramatic spectral inversion is observed upon melting. This suggests a conformational alteration in the vicinity of the pyrenyl moiety. To ascertain that the observed effect is not due to the intercalative binding of tetraols as consequences of possible thermal degradation and photodegradation of the adducts, a CD spectrum of a 0.1 mM DNA solution containing 9.2 μM tetraols derived from (+)-*anti*-BPDE was made. No detectable induced pyrenyl CD spectrum was observed. These results are, thus, consistent with the notion that orientations of the pyrenyl moieties with respect to the DNA bases are grossly different before and after melting (and subsequent cooling). In contrast, the pyrenyl CD spectrum for the (−)-*anti*-BPDE-modified DNA exhibits a very weak broad positive feature, a consequence of the heterogeneous and much reduced covalent modification. Although an intensity reduction is evident in the postmelt spectrum of the (−) adducts, no CD sign inversion is observed (results not shown).

Fluorescence Emission Spectra. Anti-BPT (hydrolysis product of *anti*-BPDE) exhibits an absorption maximum at 343 nm when free in aqueous solution. The emission spectrum of this compound exhibits maxima at 379 and 399 nm upon excitation at 343 nm. If the excitation wavelength is changed to 353 or 260 nm, these same maxima are still apparent, albeit with considerably reduced intensities (20-fold and 5-fold, respectively). Physical binding of *anti*-BPT to DNA results in near complete quenching of the pyrenyl fluorescence (Ibanez et al., 1980).

Consistent with dominant external binding characteristics, the (+)-*anti*-BPDE covalently bound to DNA also exhibits 379- and 339-nm emission maxima (Figure 3A) when excited at 343 or 346 nm. Excitation at the intercalative absorption band, at 353 nm, results in a reduction of fluorescence intensity as expected, due to the lack of an absorbance maximum or shoulder at this wavelength. The relative intensity reduction is only about 4-fold, contrasting to the 20-fold reduction in free *anti*-BPT. This difference is due in part to the slight red shifts (2–3 nm) of the absorption spectra of the covalently bound adducts, and second, to the fluorescence contribution of the minor intercalative covalent adducts. This is in contrast to the complete fluorescence quenching resulting from physical binding of *anti*-BPT. This is evidenced by the slight red shift observed in the emission spectrum when the excitation is placed at 353 nm. It is interesting to note that excitation at the 260-nm DNA absorption region results in only slightly lower intensity than that of 343-nm excitation (in contrast to a 5-fold reduction in the case of *anti*-BPT) and a discernible red shift.

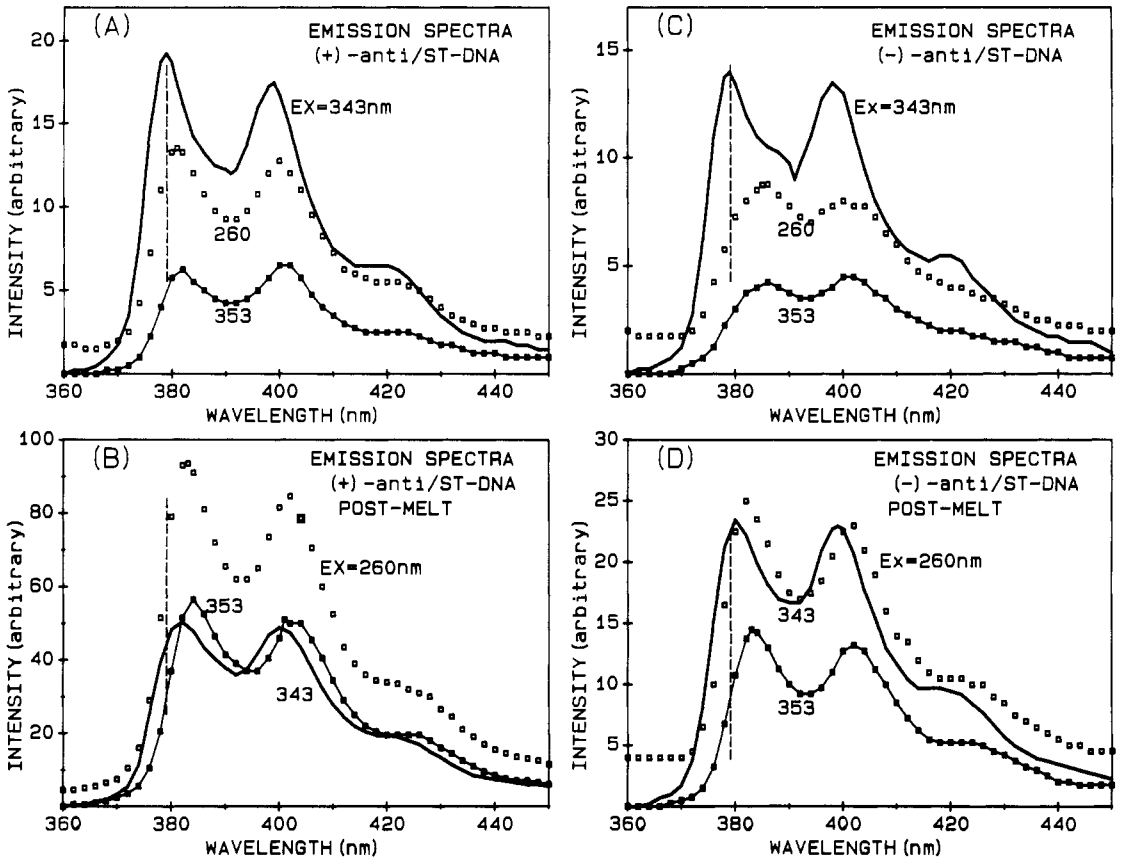

FIGURE 3: Fluorescence emission spectra at room temperature of (+)- and (−)-*anti*-BPDE-modified ST-DNA before (A and C) and after (B and D) thermal denaturation. The dashed lines are 379-nm wavelength markers.

This red shift is identical with that of 353-nm excitation.

Upon melting and cooling, however, dramatic fluorescence intensity enhancement is observed upon excitation at 353 or 260 nm. The emission resulting from excitation at 353 nm is slightly higher than that of excitation at 343 nm and shows an apparent red shift of the maxima (Figure 3B). The fluorescence due to the 260-nm excitation is twice as intense as that observed at the 343-nm excitation, with wavelengths for the emission maxima (the red shifts are readily apparent) again identical with those from excitation at 353 nm. These fluorescence features are consistent with the interpretation that stacking interactions of the (+)-*anti*-BPDE moiety with the DNA bases predominate upon thermal denaturation and subsequent cooling. The dramatic fluorescence enhancement and spectral red shift with 260-nm excitation are consistent with the notion that significant fluorescence originates via a nonradiative energy transfer from DNA bases to the pyrenyl moieties due to stacking. The dominant stacking contribution after melting also manifests itself in a slight red shift observed in the emission spectrum even from the 343-nm excitation.

Although the qualitative features and the relative fluorescence intensities for the (−)-*anti*-BPDE adducts prior to melting are very similar to those of the (+) enantiomer (compare panels A and C of Figure 3), the emission spectral red shifts resulting from excitation at 353 and 260 nm are prominent in the (−)-*anti*-BPDE adducts. The increased stacking interactions between the (−)-*anti*-BPDE moiety and the bases after melting are again evidenced by the enhanced emission intensities with the 353-nm excitation (Figure 3D). In contrast to those of the (+) enantiomer, however, these fluorescence intensities are still somewhat less than those of 343-nm excitation. The fluorescence intensities due to the 260-nm excitation are only slightly greater than those of 343-nm excitation, which contrasts with the 2-fold enhancement observed in the case of the (+) enantiomer. Those observations are consistent with the absorption spectral results indicating that the (−) modifications exert less irreversible character on the adduct renaturation at the binding sites.

Fluorescence Excitation Spectra. Since excitation at the 353-nm intercalative band results in a fluorescence maximum at 384–387 nm (in contrast to the 379-nm emission maximum observed when exciting at 343 nm), the excitation spectrum observed from monitoring the emission in the 384–387-nm region should emphasize the spectral features resulting from intercalative or stacking interactions. Prior to melting, the excitation spectra of the (+)-*anti*-BPDE adducts exhibit 345-nm maxima regardless of whether emission is monitored at 379 or 387 nm (Figure 4A). These data suggest that the contributions from the intercalative mode of binding are minor. The postmelt excitation spectrum, however, exhibits a prominent 355-nm contribution even when emission is monitored at 379 nm (Figure 4B). The excitation spectrum resulting from an emission wavelength of 387 nm results in a 355-nm maximum that is more intense than that at 345 nm, which now exists merely as a shoulder. The excitation spectra again support the findings from absorption and emission observations that stacking interactions predominate after thermal denaturation and renaturation.

The premelt excitation spectrum for the (−) adducts is very similar to that of (+) enantiomer when 379-nm emission is monitored. However, a 355-nm shoulder is clearly evident when the excitation spectrum is measured with 387-nm monitoring (Figure 4C). These data are consistent with the increased relative importance of intercalative contribution for the (−) adducts. Although melting of the (−)-*anti*-BPDE-modified DNA does not result in spectral changes as dramatic as those of the (+) counterpart, increased stacking contribution upon melting can be seen from the relative prominence of the

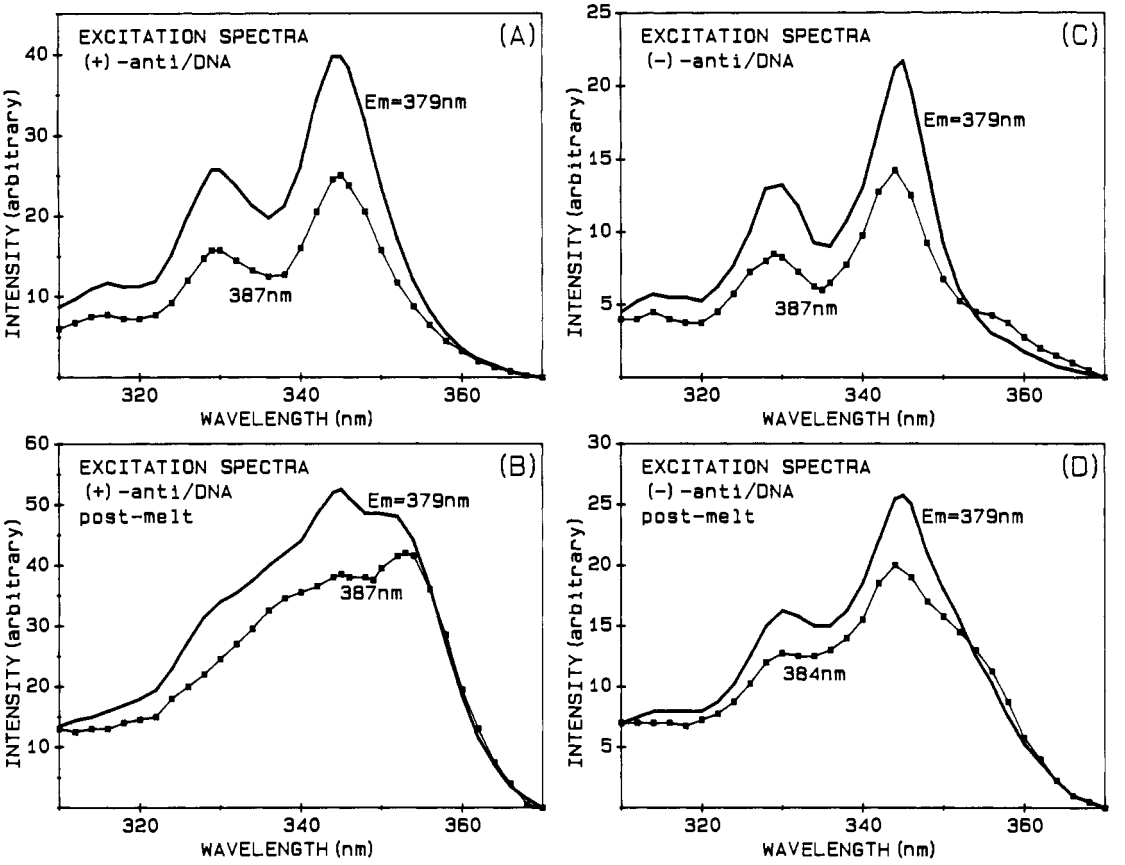

FIGURE 4: Fluorescence excitation spectra at room temperature of (+)- and (−)-*anti*-BPDE-modified ST-DNA before (A and C) and after (B and D) thermal denaturation.

355-nm shoulder in both 379- and 384-nm monitoring (Figure 4D).

Anti-BPDE-Modified Polynucleotides

Poly(dA-dT)·Poly(dA-dT) and Poly(dA)·Poly(dT). Absorption spectra for the premelt and melted *anti*-BPDE-modified poly(dA-dT)·poly(dA-dT) are shown in Figure 5. It is particularly noteworthy that, in contrast to the 345-nm maximum exhibited by the *anti*-BPDE-modified DNA, the modified poly(dA-dT)·poly(dA-dT) exhibits 353-nm maxima which show substantial hyperchromic effects and blue shifts upon melting (Figure 5). These observations are consistent with the predominant intercalative covalent binding of *anti*-BPDE in this alternating A·T copolymer (Chen, 1986). Only minor absorbance increase is observed upon melting of either the (+)- or (−)-*anti*-BPDE-modified poly(dA)·poly(dT), both of which exhibit weak broad maxima around 349 nm for the premelt solutions (results not shown). The reversible renaturation of these two polymers is evidenced by the nearly identical pre- and postmelt spectra in both DNA and pyrenyl spectral regions (not shown).

Poly(dA-dC)·Poly(dG-dT) and Poly(dA-dG)·Poly(dC-dT). The premelt absorption spectra for the (+)- and (−)-*anti*-BPDE-modified poly(dA-dC)·poly(dG-dT) and poly(dA-dG)·poly(dC-dT) exhibit 346-nm maxima. Melting of the (+)-*anti*-BPDE adducts does not greatly affect the spectra except for the slight pyrenyl hyperchromic effect for poly(dA-dC)·poly(dG-dT) and hypochromic effect with slight red shift for poly(dA-dG)·poly(dC-dT) (not shown). However, both polymers exhibit nearly complete renaturation upon cooling. In contrast, the pyrenyl spectra for the (−)-*anti*-BPDE modification exhibit 355-nm maxima, indicative of important intercalative contributions (Chen, 1986). This interpretation is supported by the much larger hyperchromic effects with

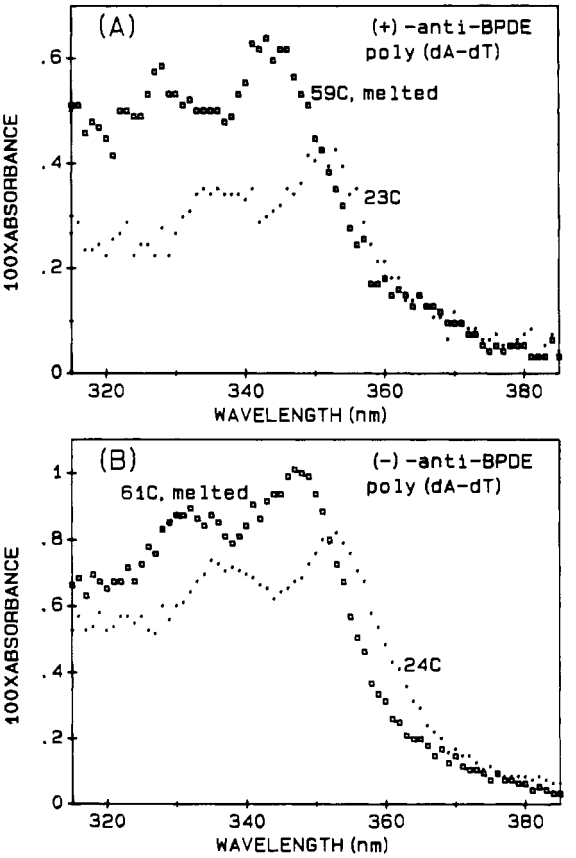

FIGURE 5: Absorption spectra of the 0.25% (+)- and 0.33% (−)-*anti*-BPDE-modified poly(dA-dT)·poly(dA-dT) (A and B) before and after thermal denaturation. The room temperature postmelt spectra are nearly identical with those of premelt spectra and are, thus, not shown.

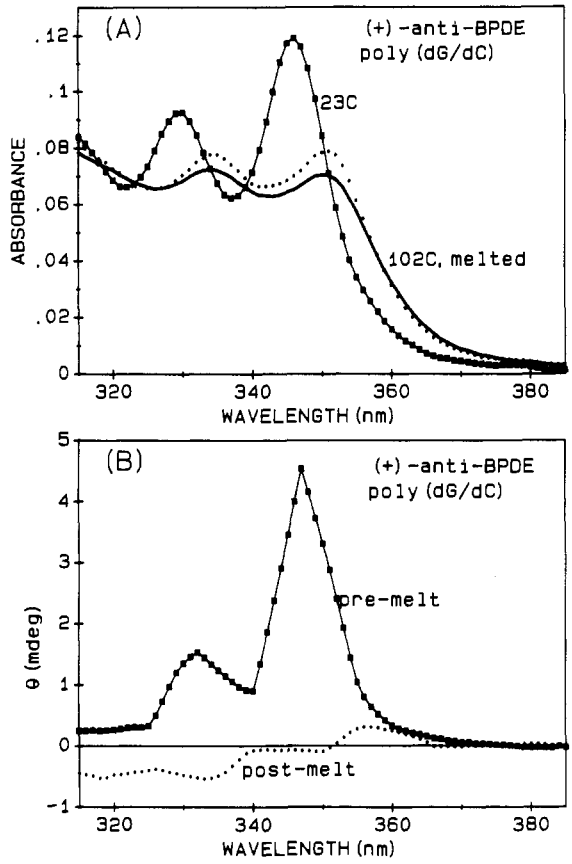

FIGURE 6: Comparison of absorption (A) and CD (B) spectra during a thermal denaturation–renaturation cycle for the 4.0% (+)-*anti*-BPDE-modified poly(dG)·poly(dC). The high temperature melted CD spectrum is similar to but smaller in magnitude than that of the postmelt room temperature spectrum.

concomitant blue shifts observed upon melting of both (−)-*anti*-BPDE-modified polymers (results not shown). Upon cooling, the long-wavelength regions exhibit complete reversibility with only slight irreversibilities observed in the 346-nm region.

Poly(dG)·Poly(dC) and Poly(dG-dC)·Poly(dG-dC). Striking nonreversible renaturation is observed in the *anti*-BPDE-modified poly(dG)·poly(dC) as shown in Figure 6. In the (+)-*anti*-BPDE adducts, a dramatic hypochromic effect with an accompanying absorption spectral red shift is seen upon melting (Figure 6A), suggesting increased stacking interactions. Upon cooling to room temperature, however, the spectral characteristics do not return to those of premelt but remain similar to those of the melted spectrum with only a slight increase in intensity.

In contrast to (+)-*anti*-BPDE, the premelt spectrum of the (−) adducts is rather broad and exhibits a hyperchromic effect upon melting, with renaturation apparently reversible at the long-wavelength region (results not shown). These observations are consistent with the interpretation of increased importance of contributions from intercalative interactions of the (−) adducts and their abilities to facilitate duplex formation.

The different adduct conformations at the binding sites for the (+) adduct modified poly(dG)·poly(dC) after denaturation are further supported by the CD measurements. The (+)-*anti*-BPDE covalently attached to duplex poly(dG)·poly(dC) initially exhibits a strong positive CD band at 348 nm. This band is completely abolished upon melting, and the resulting spectrum upon subsequent cooling is quite weak (a broad positive maximum at 355 nm), showing no resemblance to the original spectrum (Figure 6B). No such effect was observed for the (+)-*anti*-BPDE-modified poly(dA-dG)·poly(dC-dT) which also exhibits a positive CD maximum at 348 nm (Chen, 1986). This is consistent with the reversible denaturation of this polymer as revealed by the absorption and fluorescence measurements. The disappearance of this strong positive CD band at the GG sequences and the negative CD contribution of the other sequences [except poly(dA-dG)·poly(dC-dT)] (Chen, 1986) thus accounts for the earlier observed CD inversion of the (+)-*anti*-BPDE-modified native DNA upon melting.

The nonreversible thermal denaturation of the *anti*-BPDE-modified poly(dG)·poly(dC), apparent from the absorption as well as CD spectral measurements, is further evidenced in the fluorescence spectra. The emission spectra for the (+)- and (−)-*anti*-BPDE-modified poly(dG)·poly(dC) at various excitation wavelengths are shown in Figure 7. Aside from the fluorescence intensity differences, fluorescence maxima resulting from excitation at various wavelengths remain roughly at 379 and 399 nm. It should be noted that fluorescence resulting from the 343-nm excitation is approximately twice as intense as that of the 260-nm excitation, which in turn is approximately twice as efficient as that of the 353-nm excitation (see panels A and C of Figure 7).

Upon denaturation and renaturation, both the relative fluorescence intensity and spectral maxima are greatly altered. Fluorescence intensities resulting from 260- and 353-nm excitations are dramatically enhanced in comparison to that of 343-nm excitation, and the spectral maxima are red-shifted by about 5 nm (panels B and D of Figure 7). The fluorescence intensities resulting from the 260-nm excitation are about twice as intense as those of 343-nm excitation, which are similar in magnitude to those of 353-nm excitation. The identical spectral red shifts resulting from both excitations at 353 and 260 nm again support the notion that the fluorescence resulting from excitation in the UV region occurs as a result of energy transfer from the DNA bases to the pyrenyl moieties. These features are consistent with the interpretation that thermal denaturation of *anti*-BPDE-modified poly(dG)·poly(dC) results in enhanced stacking interactions. The appearance of excimer-like emission at the long-wavelength region (~480 nm) is indicative of significant stacking interactions between neighboring *anti*-BPDE moieties.

Greater postmelt stacking interactions for *anti*-BPDE covalently bound to poly(dG)·poly(dC) are also evident from the comparison of pre- and postmelt fluorescence excitation spectra (Figure 8). Since fluorescence at 384 nm is derived mainly from the stacked moieties, excitation spectra obtained by monitoring at this wavelength should emphasize stacking features. Indeed, the postmelt excitation spectra for the (+)- and (−)-*anti*-BPDE-modified poly(dG)·poly(dC) reveal prominent 355-nm shoulders when emission at 384 nm is monitored (see panels B and D of Figure 8).

The thermal denaturation–renaturation characteristics of the (+)-*anti*-BPDE-modified poly(dG-dC)·poly(dG–dC) are complicated by its higher than 100 °C melting temperature as well as possible DNA degradation at high temperatures. However, alkaline and acid denaturation experiments indicate that poly(dG-dC)·poly(dG-dC) is less susceptible to nonreversible renaturation resulting from covalent modifications (results not shown). In these experiments, the exposure time to an acid or a base has been kept to a minimum in order to reduce the chance of DNA or adduct degradation.

Discussion

Evidence from spectroscopic measurements presented in this paper strongly suggests that the adduct conformations at the

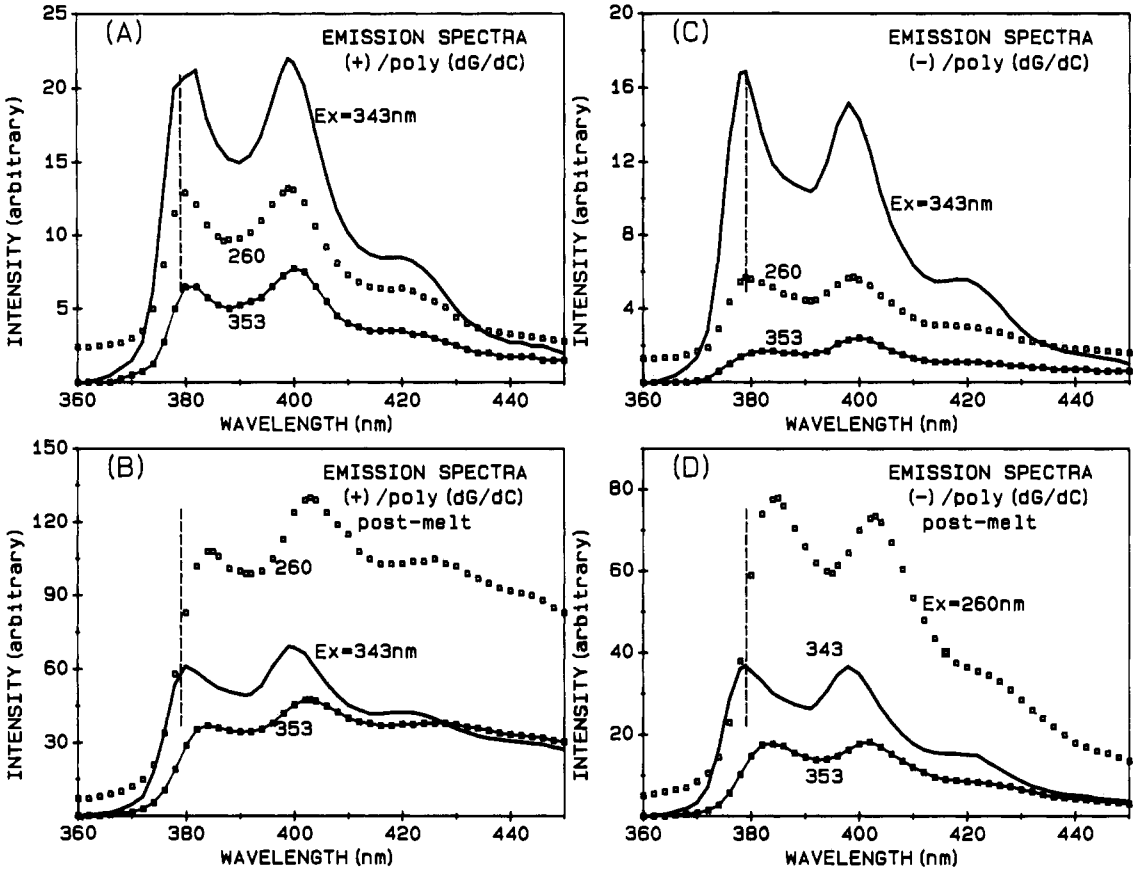

FIGURE 7: Pre- and postmelt fluorescence emission spectra at room temperature of the (+)-*anti*-BPDE (A and B) and (-)-*anti*-BPDE (C and D) modified poly(dG)·poly(dC).

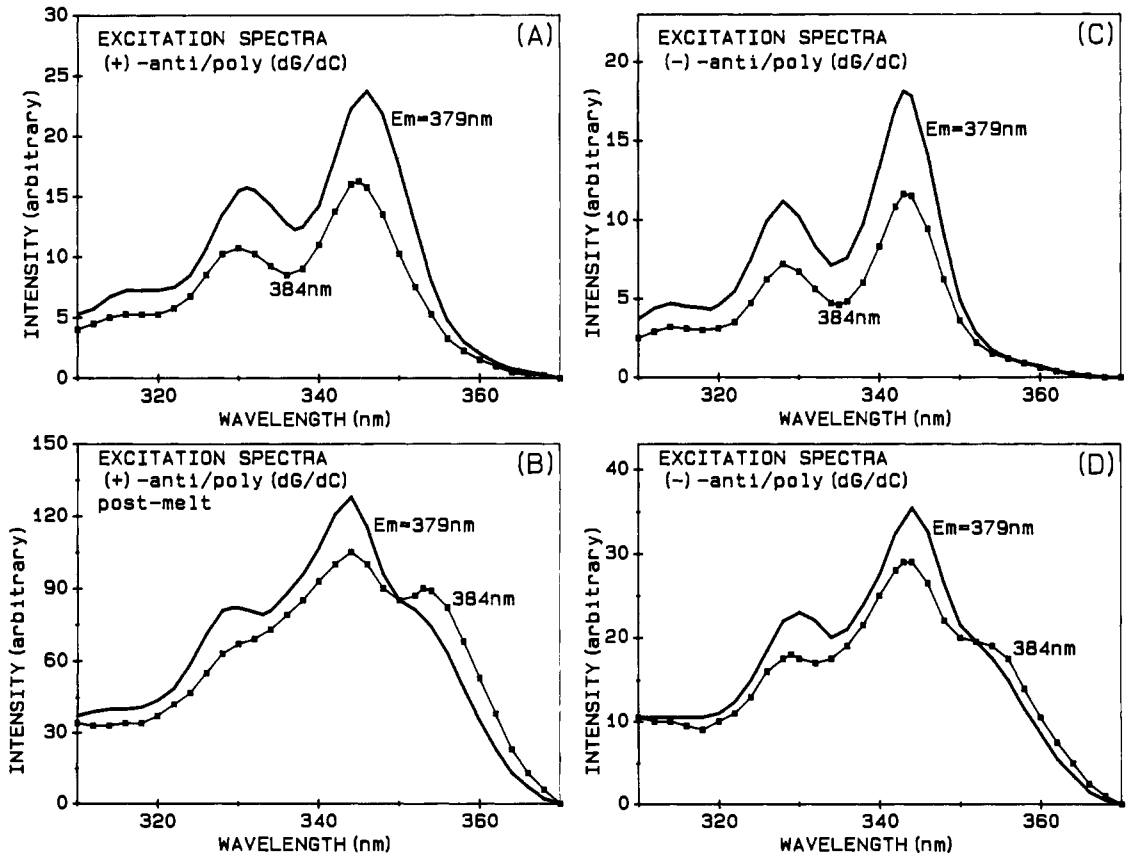

FIGURE 8: Room temperature pre- and postmelt fluorescence excitation spectra of the (+)-*anti*-BPDE (A and B) and (-)-*anti*-BPDE (C and D) modified poly(dG)·poly(dC).

binding sites are grossly different before and after thermal denaturation of the (+)-*anti*-BPDE-modified DNAs. Although interpretation of the results is complicated by the incomplete reannealing of the thermally melted DNA, the finding that the postmelt spectral characteristics of (+)-*anti*-BPDE-modified native DNA exhibit significant stacking interactions, in contrast to those of premelt adducts, is in conformity with the conclusion reached by other spectroscopic evidence (Geacintov et al., 1976, 1978, 1980; Lefkowitz & Brenner, 1982) indicating that the covalently bound (+)-*anti*-BPDEs in native DNA are predominantly external in nature. The inability to return to the premelt adduct conformation at the binding sites of negligible stacking interactions appears to conflict with the premise that these original externally bound moieties are the result of reorientation of the intercalated *anti*-BPDE. Such a mechanism most likely would involve local denaturation–renaturation at the vicinity of the binding sites and should result in the more stable stacking conformations.

Results from the polynucleotide studies further reveal that the (+)-*anti*-BPDE-modified poly(dG)·poly(dC) exhibits the greatest nonreversible denaturation at the binding sites. This, coupled with the previous findings that this polymer suffers the most extensive (+)-*anti*-BPDE modification (Chen, 1985a, 1986), suggests that $(dG)_n$·$(dC)_n$ regions may be responsible for such observed effects in native DNA. The ability to form stacked conformations in the single-strand dG stretch and the preference of pyrenyl moieties to stack with guanine may in part be responsible for this effect.

The inability for the DNA to renature to the original adduct conformations at the covalent binding sites may have important implications for DNA replication and transcription processes and, consequently, for the actual mechanisms of carcinogenesis. Studies by Leffler et al., (1977) have shown that, with increasing levels of *anti*-BPDE covalent modification, there is progressive inhibition of transcription. The finding that the $(dG)_n$·$(dC)_n$ regions exhibit the greatest adduct conformational differences between the renatured and the premelt ones may be of significance, as long homopurine–homopyrimidine sequences exhibiting hypersensitivity of the S1 endonuclease often flank genes in eucaryotic DNA. In this connection, it is of particular interest to note that, of the two protein binding regions within the hypersensitive domain of β-globin gene, one contains $d(G)_{15}$·$d(C)_{15}$ and the other contains a large number of shorter GG sequences (Emerson et al., 1985). In fact, Boles and Hogan (1986) recently described a photochemical technique for mapping the covalent binding sites of *anti*-BPDE within DNA from the transcription control region of the chicken adult β-globin gene. They found that this region contains highly preferred *anti*-BPDE binding sites and suggested that long poly(dG) sequences should be the preferred sites for BPDE action in other genes.

Although the precise structure of the stacking conformation of *anti*-BPDE in single-strand DNA is not known, it most likely resembles the stacked conformation of *anti*-BPDE-modified dinucleoside monophosphate (Frenkel et al., 1978), in which the covalently attached *anti*-BPDE stacks with the neighboring base by an anti to syn rotation of the modified guanine residue about its glycosidic bond. Such a model is quite reasonable, as base rotation about its glycosidic bond is much easier for the single strand than for the duplex form. The prominent hypochromic effect exhibited by the (+)-*anti*-BPDE-modified homopurine–homopyrimidine polymers [poly(dG)·poly(dC) and poly(dA-dG)·poly(dC-dT)] upon melting, thus, appears to suggest that stacking with the neighboring purine is an important driving force.

The fact that the (+)-*anti*-BPDE-modified poly(dA-dG)·poly(dC-dT) renatures reversibly at the binding sites while poly(dG)·poly(dC) does not may partly be the consequence of stacking interactions for the latter between the contiguously bound pyrenyl moieties in single strands. This interpretation is supported by the observed excimer-like emission spectra of the *anti*-BPDE-modified poly(dG)·poly(dC) and the ease with which this homopolymer can form unusual conformations.

Our evidence also indicates that the nonreversible renaturation at the covalent binding sites for the (−)-*anti*-BPDE adducts is somewhat less pronounced. This may be due to the greater intercalative contributions of the (−) adducts which return to the original premelt conformations upon denaturation–renaturation, although the lower level of covalent modification is certainly a factor. The greater relative intercalative covalent contribution of the (−) adducts is evident from the appearance of a shoulder or broadening in the 353-nm region of the premelt absorption spectra and the hyperchromic effect accompanied by concomitant blue shifts upon melting. The reduced nonreversibility coupled with the lower level of covalent modification by the (−) enantiomer may impart the lower carcinogenic activity of this isomer.

Results of these denaturation studies also appear to support the notion that intercalative physical binding may lead to the formation of intercalative covalent adducts and that the externally bound covalent adducts are derived from external bimolecular encounters. Due to relative rigidity of the duplex structure, nonintercalated pyrenyl moieties are prevented from stacking with the bases. However, once the duplex is melted, the pyrenyl moiety can stack with the bases to attain the thermodynamically more favorable conformation.

Indeed, physical binding studies of pyrene (Chen, 1983), BP-diol (Yang et al., 1983) and *anti*-BPT (Chen, 1984) with polynucleotides have revealed that intercalative binding is much more preferred in poly(dA-dT)·poly(dA-dT) than any guanine-containing polymers. Covalent binding studies of *anti*-BPDE to polynucleotides also suggest that only poly(dA-dT)·poly(dA-dT) exhibits predominant intercalative covalent lesion and the lowest level of modification (Chen, 1986). It is of particular interest to note that a recent study on the noncovalent physical binding of *anti*-BPDE to synthetic polynucleotides (Moussaoui, 1985, Geacintov, 1986) has revealed that the order of intercalative binding is poly(dA-dT)·poly(dA-dT) $\gg$ poly(dG-dC)·poly(dG-dC) $>$ poly(dG)·poly(dC) $>$ poly(dA)·poly(dT). Thus, it is reasonable to suggest that, in native DNA, intercalative physical binding of *anti*-BPDE occurs mainly at pyrimidine–purine sequences, especially dT-dA [theoretical calculation indicates that this is the most preferred sequence and intercalative binding at the dA-dT sequence is energetically less favorable (Miller et al., 1985)], and covalent lesions occur mainly at the guanine-containing sequences via external bimolecular encounters at the minor groove.

How does one then reconcile (without imposing the notion of adduct reorientation) the fact that the physical binding of (+)-*anti*-BPDE to native DNA is predominantly intercalative while the covalent adducts are substantial and predominantly external in nature? The likely explanation appears to be that the physical binding of *anti*-BPDE to DNA is predominantly intercalative in nature due to the high [DNA]/[BPDE] ratio used in the experiments but that the binding sites are less likely to react covalently (possbily due to intercalative preference at the dT-dA and other pyrimidine–purine sites and unfavorable geometric orientation of the reactive groups for the

low-energy intercalated conformations). Consequently, many exchanges between the intercalated and nonintercalated sites occur during the lifetime of an *anti*-BPDE (Geacintov, 1985), and the external nature of the covalent adducts can be rationalized in terms of higher covalent reactivity at the external sites (dG-containing sequences). The experimental evidence suggests that the time constant for the release of the intercalated *anti*-BPDE is much shorter than the characteristic time for the covalent formation (Meehan & Bond, 1984; Geacintov, 1985).

It may be of interest to note that a theoretical model (Miller, 1985) has been proposed to rationalize the external nature of (+)-*anti*-BPDE covalent adducts in terms of an anti to syn rotation about the glycosidic bond after covalent lesion at the intercalation site. Although such a model appears to be quite reasonable, it would predict a facilitation of a B to Z transition through (+)-*anti*-BPDE modification, as guanosine exists as a syn conformation in the Z form. Our previous studies (Chen, 1985b) as well as others (Moussaoui et al., 1985) on the (+)-*anti*-BPDE-modified poly(dG-dC)·poly(dG-dC), however, suggest inhibition of B to Z transformation in the covalently bound regions.

Finally, it is also worth noting that although we have characterized the guanine binding sites exhibiting slight red shifts as "external", Hogan et al. (1981) have presented evidence to argue that the *anti*-BPDEs are intercalated in "wedge-like" fashion at these sites.

ACKNOWLEDGMENTS

I thank Drs. D. Graves and H. Van Woert for their comments and careful reading of the manuscript.

Registry No. (+)-*anti*-BPDE, 63323-29-5; poly(dG)·poly(dC), 25512-84-9; (−)-*anti*-BPDE, 63357-09-5; poly(dA-dT), 26966-61-0; poly(dA)·poly(dT), 24939-09-1; poly(dA-dC)·poly(dG-dT), 55684-99-6; poly(dA-dG)·poly(dC-dT), 36833-12-2; poly(dG-dC), 36786-90-0.

REFERENCES

Boles, T. C. & Hogan, M. E. (1986) *Biochemistry 25*, 3039–3043.

Brookes, P., & Osborne, M. R. (1982) *Carcinogenesis (London) 3*, 1223–1226.

Chen, F.-M. (1983) *Nucleic Acids Res. 11*, 7231–7250.

Chen, F.-M. (1984) *Carcinogenesis (London) 5*, 753–758.

Chen, F.-M. (1985a) *Biochemistry 24*, 5045–5052.

Chen, F.-M. (1985b) *Biochemistry 24*, 6219–6227.

Chen, F.-M. (1986) *J. Biomol. Struct. Dyn. 4*, 401–418.

Conney, A. H. (1982) *Cancer Res. 42*, 4875–4917.

Emerson, B. M., Lewis, C. D., & Felsenfeld, G. (1985) *Cell (Cambridge, Mass.) 41*, 21–30.

Frenkel, K., Grunberger, D., Boublik, M., & Weinstein, I. B. (1978) *Biochemistry 17*, 1278–1282.

Geacintov, N. E. (1985) in *Polycyclic Hydrocarbons and Carcinogenesis* (Harvey, R. G., Ed.) ACS Symp. Ser. No. 283, pp 107–124, American Chemical Society, Washington, DC.

Geacintov, N. E. (1986) *Carcinogenesis (London) 7*, 759–766.

Geacintov, N. E., Prusik, T., & Khosrofian, J. M. (1976) *J. Am. Chem. Soc. 98*, 6444–6452.

Geacintov, N. E., Gagliano, A., Ivanovic, V., & Weinstein, I. B. (1978) *Biochemistry 17*, 5256–5262.

Geacintov, N. E., Ibanez, V., Gagliano, A. G., Yoshida, H., & Harvey, R. G. (1980) *Biochem. Biophys. Res. Commun. 92*, 1335–1342.

Geacintov, N. E., Yoshida, H., Ibanez, V., & Harvey, R. G. (1981) *Biochem. Biophys. Res. Commun. 100*, 1569–1577.

Geacintov, N. E., Ibanez, V., Gagliano, A. G., Jacobs, S. A., & Harvey, R. G. (1984) *J. Biomol. Struct. Dyn. 1*, 1473–1483.

Harvey, R. G. (1981) *Acc. Chem. Res. 14*, 218–226.

Hogan, M. E., Dattagupta, N., & Whitlock, J. P., Jr. (1981) *J. Biol. Chem. 256*, 4504–4513.

Ibanez, V., Geacintov, N. E., Gagliano, A. G., Brandimarte, S., & Harvey, R. G. (1980) *J. Am. Chem. Soc. 102*, 5661–5666.

Jeffrey, A. M., Weinstein, I. B., Jennette, K. W., Grzekowiak, K., Nakanishi, K., Harvey, R. G., Autrup, H., & Harris, C. (1977) *Nature (London)* 348–350.

Leffler, S., Pulkrabek, P., Grunberger, D., & Weinstein, I. B. (1977) *Biochemistry 16*, 3133–3136.

Lefkowitz, S. M., & Brenner, H. C. (1982) *Biochemistry 21*, 3735–3741.

MacLeod, M. C., & Selkirk, J. K. (1982) *Carcinogenesis (London) 3*, 287–292.

Meehan, T., & Straub, K. (1979) *Nature (London) 277*, 410–412.

Meehan, T., & Bond, D. M. (1984) *Proc. Natl. Acad. Sci. U.S.A. 81*, 2635–2639.

Meehan, T., Camper, H., & Becker, J. F. (1982) *J. Biol. Chem. 257*, 10479–10485.

Miller, K. J., Taylor, E. R., & Dommen, J. (1985) in *Polycyclic Hydrocarbons and Carcinogenesis* (Harvey, R. G., Ed.) ACS Symp. Ser. No. 283, pp 239–288, American Chemical Society, Washington, DC.

Moore, P. D., Koreeda, M., Wislocki, P. G., Levin, W., Cooney, A. H., Yagi, H., & Jerina, D. M. (1977) *ACS Symp. Ser. No. 44*, 127–154.

Moussaoui, K. M. (1985) Ph.D. Thesis, New York University.

Moussaoui, K. M., Geacintov, N. E., & Harvey, R. G. (1985) *Biophys. Chem. 22*, 285–297.

Newbold, R. F., Brookes, P., & Harvey, R. G. (1979) *Int. J. Cancer 24*, 203–209.

Undeman, O., Lycksell, P. O., Graslund, A., Astlind, T., Ehrenberg, A., Jernstrom, B., Tjerneld, F., & Norden, B. (1983) *Cancer Res. 43*, 1851–1860.

Weinstein, I. B., Jeffrey, A. M., Jennette, K. W., Blobstein, S. H., Harvey, R. G., Harris, C., Autrup, H., Kasai, H., & Nakanishi, K. (1976) *Science (Washington, D.C.) 193*, 592–595.

Yang, N. C., Hrinyo, T. P., Petrich, J. W., & Yang, D. H. (1983) *Biochem. Biophys. Res. Commun. 114*, 8–13.